Technical Report Rico 2018

Prepared by Lucila Dunnington

In cooperation with Masami Nakagawa & Meghan Helper

June 26, 2018

Rico Geologic and Geothermal Setting

The Rio Grande Rift cuts through Colorado southeast to northwest. It imparts on Colorado a thinner continental crust, steep faults, and graben fill features. These three aspects of a rift system together create ideal conditions for geothermal in certain areas of Colorado. The San Juan Rift, an adjacent rift system is the setting of Rico's geothermal. The geothermal manifests as hot spring wells that are apparent north of downtown and south of the settling ponds. Other wellbores, drilled at the service of mining companies, have discovered higher than usual geothermal gradients. Whereas the average geothermal gradient of the earth's crust is 25 degrees Celsius per kilometer of depth, Rico's northern area averages geothermal gradients of 101.2 degrees Celsius per kilometer (Figure 1).

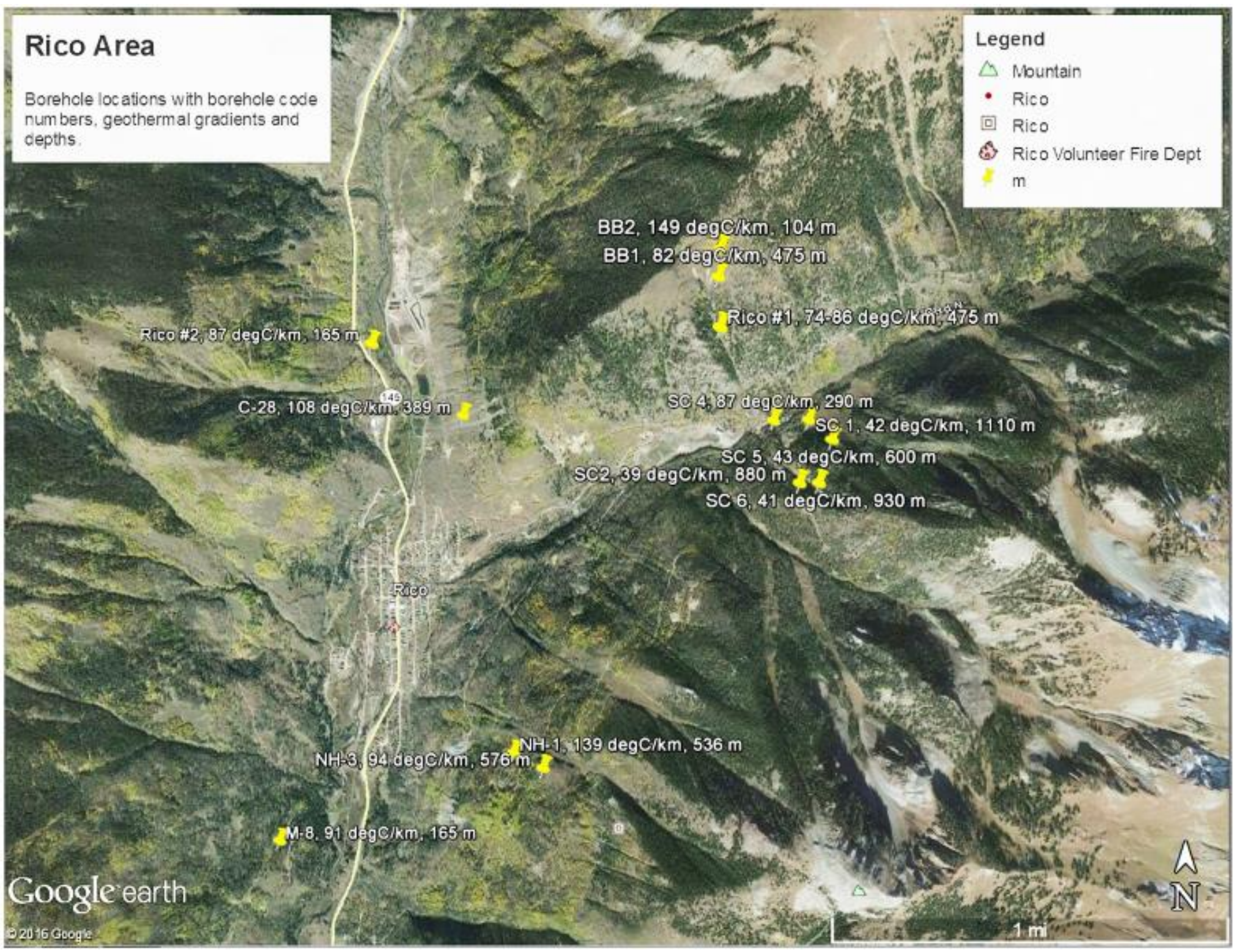

Figure 1 Wellbore data from mining exploration in Rico, CO with well identification numbers, depths and geothermal gradients

Another cluster of higher geothermal gradients (91-139 degC/km) south of Rico corresponds to old mine sites in the area: the Jones, Lexington, and Enterprise Mines. One mining company reported water from a well reaching temperatures of 114 degrees Celsius (Medlin, 1983).

The hydrothermal system that produced the enhanced geothermal gradient four million years ago likely followed older paths carved out by 65 million year old latite porphyries. These porphyries enrich the exposed geothermal water with iron, while the underlying Leadville Limestone gives the water its notable calcium carbonate signature.

Table 1 Metals and nonmetals in mg/L from Rico's three sampled hot springs (BDL indicates the measurement fell below detection limits).

Analyte	HS North	HS East	HS West
Boron	0.191363	0.132166	0.083106
Barium	0.025925	0.027909	0.034358
Beryllium	0.006216	0.005905	0.005445
Calcium	735.5724	699.691	648.9356
Cadmium	BDL	BDL	BDL
Cobalt	0.00073	0.000849	0.001148
Chromium	BDL	BDL	BDL
Copper	BDL	BDL	BDL
Iron	6.814743	5.375104	5.012546
Potassium	24.22891	24.3021	24.55809
Lithium	0.189954	0.187357	0.200981
Magnesium-279	78.91686	80.18077	80.73418
Magnesium-285	90.12084	89.65709	88.37058
Manganese	1.329997	1.112805	1.030429
Sodium	75.30716	71.81082	65.97644
Nickel	BDL	BDL	BDL
Phosphorus	0.020248	BDL	0.011906
Lead	BDL	BDL	BDL
Sulfur	264.4226	233.9239	226.4177
Selenium	0.031145	0.021302	0.026239
Silicon	49.09253	44.86067	46.78174
Strontium	10.17675	9.176513	7.956065
Thallium	BDL	BDL	BDL
Vanadium	BDL	BDL	BDL
Zinc	0.030006	0.047398	0.100093
Tin	BDL	BDL	BDL
Molybdenum	0.002769	0.003028	0.004633
Antimony	BDL	BDL	BDL
Titanium	BDL	BDL	BDL

Table 2 Anion report on Rico hot springs in mg/L

	Fluoride	Chloride	Sulfate
HS North	2.94	4.72	1009.29
HS West	1.68	3.67	1134.41
HS East	2.80	5.25	512.55

While many natural geothermal hot springs are radioactive, a 2016 result from accredited lab, ALS in Fort Collins, showed Rico water to be 11 ± 2.8 pCi/L, lower than Glenwood Springs (27 pCi/L) and Radium Hot Springs (17 pCi/L) in Colorado (Appendix A.3). The main elemental breakdown of the Rico Hot Spring water can be seen in Tables 1 and 2 (From 2015 sampling on Colorado School of Mines ICP-MS).

Previous researchers (and bathers at Rico's springs) have noted that Rico's geothermal resources are mixed with rain or surface water. In a dry season, the spring's temperature can elevate 1 or 2 degrees Celsius from its average of 42 degrees. Geophysics conducted in the early 2010's show that the Last Chance fault, located on the northern side of the Rico Dome (just south of the C-dot station, oriented east-west), is a major conduit introducing water to the deeper heat source. SP, resistivity, thermoluminescence, and geochemistry studies from 2015 to 2016 suggest that once the water enters the Last Chance Fault, it flows south to north in the subsurface.

2016 Geophysics

In 2016, team geologists found a site for a resistivity survey approximately two miles north of the Town of Rico, where a resistivity line of 720 meters could cross two of the three identified fault structures associated with the Blackhawk Fault. The southernmost and middle expression of the Blackhawk fault were identified in the resistivity data inversion (Appendix A.4; Figure A5).

A resistive mass was identified about 43 meters deep from the surface on the northern side of the Blackhawk Fault. This northern resistive mass could provide a northern boundary for the geothermal reservoir at Rico, forcing the warm waters upwards as the subsurface currents travel northward. If the resistive feature at the Blackhawk Fault is indeed the northern boundary for the Rico reservoir, then, assuming a continuous reservoir from the Rico Dome to the Blackhawk, Rico's reservoir's areal extent is about 1 square mile, double the previous estimate made by looking solely at surface expressions (Pearl, 1972).

Objectives of 2018

The task for the geophysics team from Colorado School of Mines during the 2018 expedition was to estimate the depth. With a depth estimate, prospective developers could plan drilling sites, estimate the volume of the reservoir and with the geothermal gradients from Figure 1, a reservoir temperature could be estimated.

Previous delineations of the reservoir suggest that the planar areal extent of Rico's reservoir was 2.5 km^2 or about 1 mi^2. The artesian pressure of Rico's springs yield 800 liters per minute on the fault of the Rico dome (Medlin, 1983). In order to sustainably manage the geothermal resource present in Rico, the amount withdrawn from the reservoir must be returned, either by a closed loop system, or by allowing adequate recharge from the surface waters. Vertical depth estimates are necessary for understanding the water budget of the geothermal system.

Similarly, reservoir temperature estimates are essential for project development. With an average geothermal gradient of 101 degC/km, if the reservoir is 400 m deep, the water will be around 40 degC, and if the reservoir is 800 m deep, the water will be 80 degC. 40 degree water can be developed into a spa like Dunton's or greenhouses like Pagosa's; while 80 degC water can be converted to electricity with the recently developed Organic Rankine Cycle binary geothermal technology.

Even though geothermal power has some of the lowest overall costs when compared to other power sources, uneven distribution of easily reached resources, high upfront costs, and uncertainty in the surface measurements have prevented it from being widely adopted (International Finance Corporation, 2013). A well-defined geophysics exploration program can help alleviate these issues. Even with the variability involved in geophysical data processing and inversion, the success rate of well drilling has been shown to increase by 30-40% when geophysical data is provided (Gray, 2011). Geophysical data inversion coupled with an understanding of the geologic setting of the geothermal reservoir helps with planning and executing successful wells. Since the cost of a typical well can be $143 per foot (increasing with depth), accounting for 30-60% of the capital investment in a geothermal power plant, proper drill planning can mitigate a major financial risk of reservoir development (Lukawski et al., 2014).

Methods

The geophysical method selected for this project based on budget and target depth was magnetotellurics (MT). Magnetotellurics can give deep resistivity estimates, to the 10 km range; the ground conditions, duration of a survey, and length of electrode cables all determine the depth the MT survey can reach at a particular site. Able to detect important features of a reservoir, including the more resistive "caprock," and less resistive faults and reservoir formation, MT has been widely used in geothermal reservoir delineations in the United States, Iceland, New Zealand, Hungary, China, Ethiopia, Peru, Australia, and India.

The MT setup generally requires a 100 m by 100 m flat expanse, set apart from electrical wires, busy roads, and other major sources of noise. At the center of the survey is a recording system (in our case an ADU-07e from Metronix), which reads the electric and magnetic fields and stores data from the long collection time (typically 6-14 hours). Four 50 m cables are reeled out from the recording system to the north, south, east and west directions. The extended ends attach to silver-silver chloride electrodes which must be buried 15-30 cm into the ground, depending on how rocky the soil is (deeper burial is required if the electrode does not have good contact with the shallow ground). Parallel and well-spaced from the electrode cables, magnetometers are placed in trenches in the ground (Figure 2).

The magnetometers collect the magnetic field from the earth's magnetosphere, and the electrodes collect the induced, associated electric field. Because the instrument has to be very sensitive to collect the magnetic field disturbances caused by solar winds and lightning, coiled wire, underground pipes, and more obvious electrical noise from cars and powerlines can produce substantial noise in the data.

The data must be pre-processed then processed in the case of noisy locations. The research group used the ProcMT program to pre-process and process the data, involving manual and programmed removal of unusual or abrupt variations in the natural curved signal. After preprocessing, the data can be “inverted,” changing the frequency data into ground resistivity information (Zond 2D MT was used for inversion). The inversion of data varies modestly with the user, since programs will smooth and dampen the data based on the perceived quality of the collection. Most programs allow the inclusion of known geological structures or well logging data, which also influences the end result.

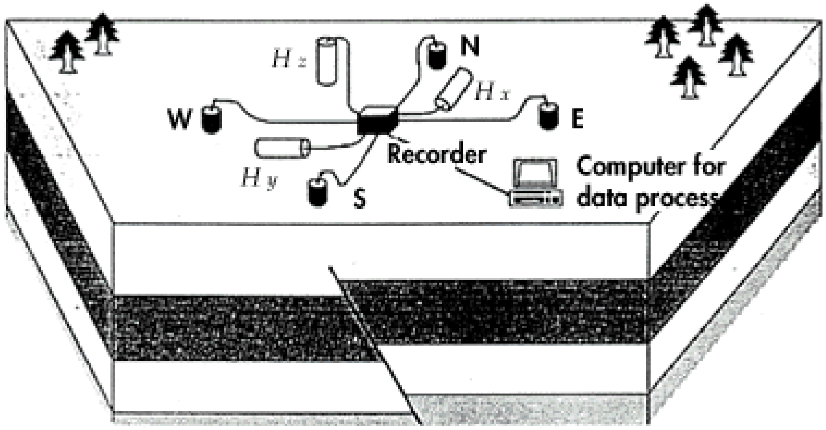

Figure 2 Top: basic schematic of MT survey layout (from seismo.geology.upatras.gr/MT.htm); Below: Actual image of equipment- long columns are magnetometers (smaller ones not used in Rico survey), orange case is recording system, short grey and yellow columns are electrodes

While eight areas were scouted as potential survey sites, only three sites were ultimately deemed suitable for the collection of MT data in Rico: the pavilion, the water tower, and the western hot spring (Figure 3). The other five locations were rejected mainly because of the noise level apparent in preliminary sampling. After a survey was set-up, a mini-survey was acquired to check that the readings had tolerable noise levels, and that good contact was made between the ground and the electrodes. If needed, deeper holes were dug for the electrodes, and sometimes a bentonite-water mixture was added to the hole to improve the contact conditions, then the mini-survey was rerun. While the recommended acquisition time for the target depth at Rico (500-1000m) is between 4 and 6 hours, the full pavilion survey acquired for 6 hours, the water tower survey acquired for 8 hours and the hot spring survey acquired for 8 hours to ensure quality depth measurements. The MT recording device registered frequencies between 0.0005 Hz and 1000 Hz, which invert to resistivities between 0.001 ohm-m and 10,000 ohm-m, an acceptable range for the expected resistivities in the subsurface of Rico.

After the data was collected, the raw data was analyzed as a time series plot to ensure it collected appropriate data throughout the survey, without egregious noise. The data was downloaded and taken back to Golden for processing. ProcMT was set to an auto-smooth setting in which data outside a coherency of 0.4 was rejected, and specific stand-alone peaks were removed. ProcMT provided the processed data as EDI files.

Then the three processed EDI files from each site were compiled on Zond 2D MT software and inverted together to produce a single 2D composite cross section, showing resistivity to a depth of 1.5 kilometers. The Marquardt inversion method was used, with 10 horizontal layers, and 20 vertical layers between sampling sites, in order to attain a fine mesh for processing. Medium depth smoothing and dampening values were used since the data had been processed and resistive boundaries were unknown. The inversion took 20 iterations to arrive at a result (for more about Marquardt inversion, see Appendix A.2).

Figure 3 MT survey sites for June 2018 Rico exploration overlaid on Google satellite image

Results

The image in Figure 4 is the composite cross section produced by the Zond 2D MT inversion. Warmer colors represent higher resistivities (lower water content) and cooler colors represent lower resistivities (higher water content). The depth represented in the inversion is 1.5 kilometers below the surface. The y-axis shows the level in kilometers above sea level. The x-axis marks the surveys and counts kilometers from the first survey point (the pavilion). The southern-most point is on the left and the northern-most point is on the right.

The top image is the original resistivity pseudo-section inferred by the square root of the period of signals received by the electrodes. The second image is the composite resistivity calculated by inversion equations, and the bottom image is the smoothed resistivity by depth image. The resistive Rico dome is the only information added to the MT data for the inversion image.

At the hot spring site (3-MT), a fault is visible, providing a less resistive conduit to a reservoir at depth. From 500 m deep to about 1000 m there is a less resistive zone that extends northward from the surveyed section. A similar pattern is observed south of the resistive feature under the pavilion. The resistivity of the subsurface appears to increase south of the pavilion site.

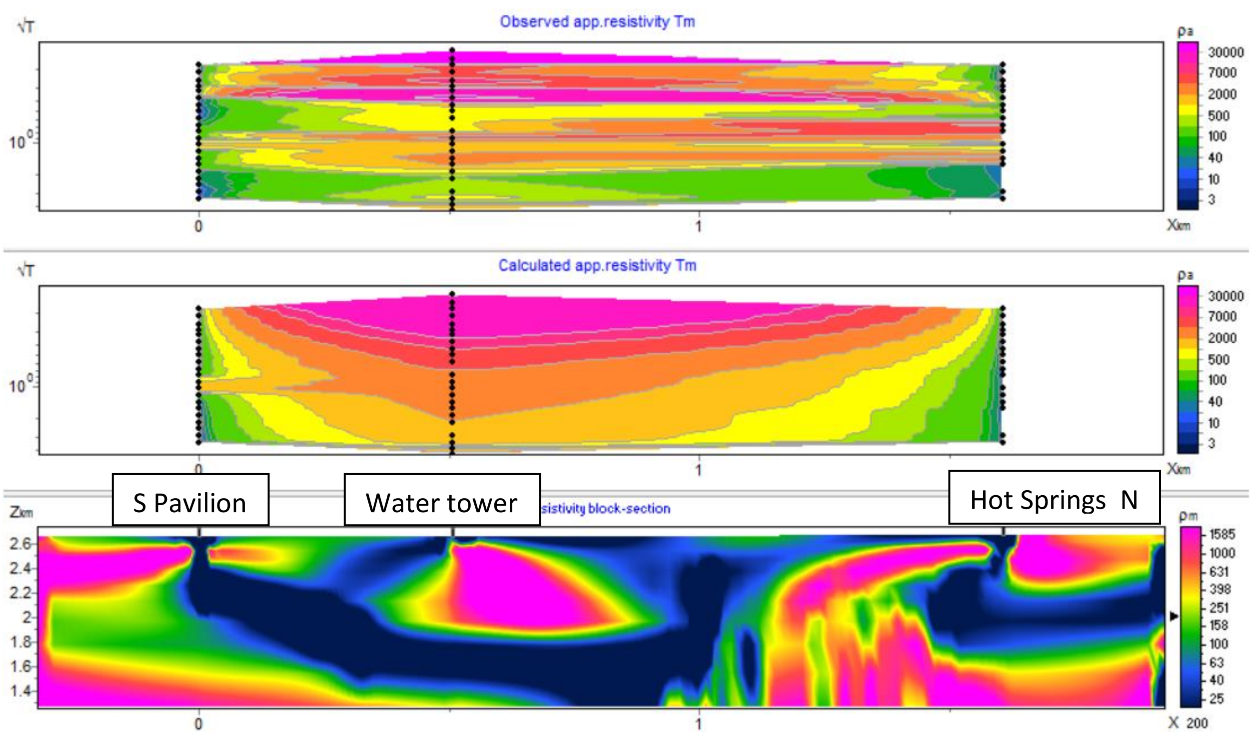

Figure 4 MT compilation and inversion of three survey sites from Zond 2D software, right is north, left is south, pink is high resistivity, blue is low resistivity, vertical axis is kilometers above sea level, horizontal axis is kilometers north of the pavilion

Several inversions were made at different smoothing factors, damping factors, and the Occam inversion method was also employed to test the sensitivity of this result. All variations show the appearance of a low resistivity zone between 500 and 1000 m directly below the hot spring survey site (see Appendix A.1).

Discussion

The depth and position of the less resistive zone north of the resistive Rico Dome correspond to the location of the Leadville Limestone, a formation which is typically bound at the top by a latite porphyry in the local geology (the orange stripe in Figure 5). The Leadville Limestone is offset by faulting all the way to the Blackhawk Fault (see light purple labeled “Ml” in cross section, Figure 5). Limestone dissolves when it comes in contact with acidic water, and thus serves as a accomodating reservoir. The high levels of calcium and bicarbonate in the hot spring water chemistry corroborate the limestone as a major storage formation. The Leadville Limestone also extends to the south where the MT shows another low resistivity zone, though less information is publicly available about the water resource potentially stored in the southern side of Rico (see well data Figure 1). The reservoir may also extend down to the Uncompahgre Quartzite (light brown “pCu” in Figure 5).

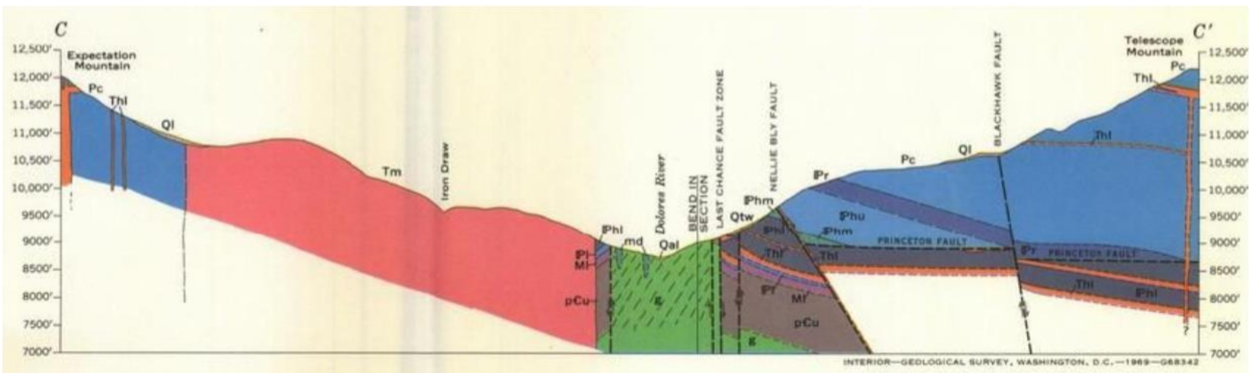

Figure 5 Geologic cross-section of Rico between Expectation Mountain and Telescope Mountain; left of the “bend in section,” the cross section extends from Expectation Mountain to the east; right of the “bend in section,” the section is oriented southwest to northeast (Telescope mountain is the northeastern-most feature) (Pratt et al., 1969)

Conclusion

The depth of a low resistivity zone detected by the MT survey corresponds to the location of the Leadville Limestone which is associated with a top confining layer: a low resistivity igneous sill. The permeable limestone, connected to the surface by a series of steep faults and capped by an impermeable rock, presents ideal conditions for a reservoir. If the Blackhawk and Last Chance faults are taken as the reservoir boundaries, and the Leadville Limestone is on average 30m thick, the water bearing reservoir is conservatively 75,000,000m^3. A 20% porosity limestone would yield 15,000,000m^3 of water. The lower depth of 800- 1000 m, using the average geothermal gradient measured at the wells, gives the north Rico water an estimated temperature of 81-101 degC, which agrees with reports from capped exploration wells of the area (Medlin, 1983).

The flowrate and temperatures potentially available at Rico are adequate for a greenhouse, spa, district heating (50-70 degC requirement), and even small scale power generation with the Organic Rankine cycle (70-100 degC requirement). A thorough economic analysis of these options is outside the scope of this report, though the corresponding non-technical report contains information on projects completed around the world, with similar resources.

References

deGroot-Hedlin & Constable. (1990) Occam's inversion to generate smooth, two-dimensional models from magnetotelluric data. http://marineemlab.ucsd.edu/resources/Pubs/OCCAM2D.pdf

Gray, David. (2011) Quantify the Economic Value of Geophysical Information. Recorder, Vol. 36 (03).

Lukawski, Maciej Z. et al. (2014). Cost analysis of oil, gas, and geothermal well drilling. Journal of Petroleum Science and Engineering, Vol. 118, 1-14.

Medlin, Eric. (1983) Modeling local thermal anomalies: constraints from conductivity, gravity and heat flow. Master of Science Thesis, University of Wyoming.

Oerter, Eric. (2010) Geothermometry of Thermal Springs in the Rico, Dunton, and West Fork Dolores River Areas, Dolores County, Colorado. Colorado Geological Survey Department of Natural Resources: Division of Minerals and Geology.

Olsen et al. (2014) Guidelines for Low-Temperature District Heating. Danish Energy Agency, EUDP 2010-II project Journal No. 64010-0479.

Pearl, Richard Howard. (1972) Geothermal Resources of Colorado. Colorado Geological Survey Department of Natural resources. State of Colorado, Denver, CO.

Pratt WP, McKnight ET & DeHon RA. (1969) Geologic map of the Rico quadrangle, Dolores and Montezuma Counties, Colorado. Department of the Interior, Geologic Quadrangle Map GQ-797.

Widodo & Saputera. (2016) Improving Levenberg-Marquardt Algorithm Inversion Result Using Singualr Value Decomposition. https://www.researchgate.net/publication/305800878_Improving_Levenberg-Marquardt_Algorithm_Inversion_Result_Using_Singular_Value_Decomposition

Appendix A

A.1 Inversion sensitivity study results

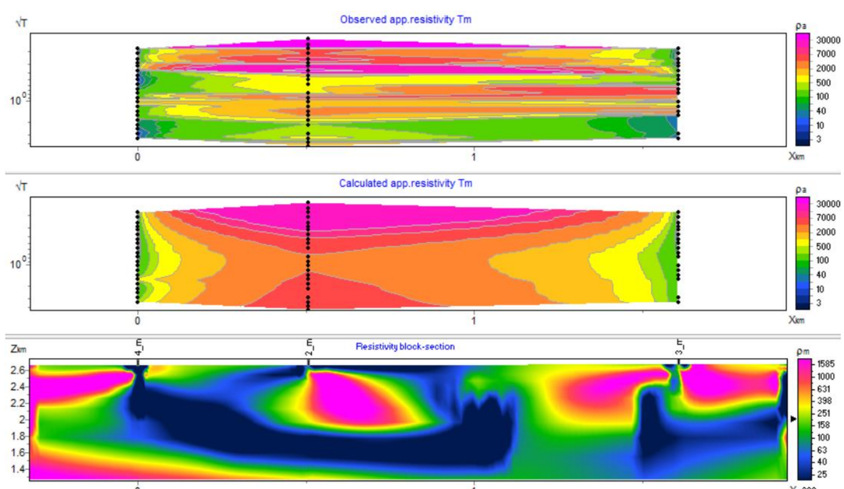

Figure A1 Processed data with dome feature added

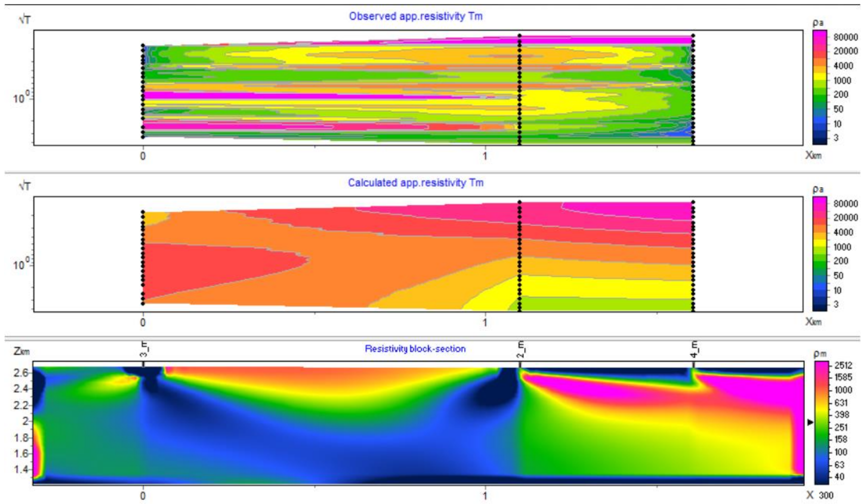

Figure A2 Unprocessed data with shadows from survey site, indicating more processing necessary

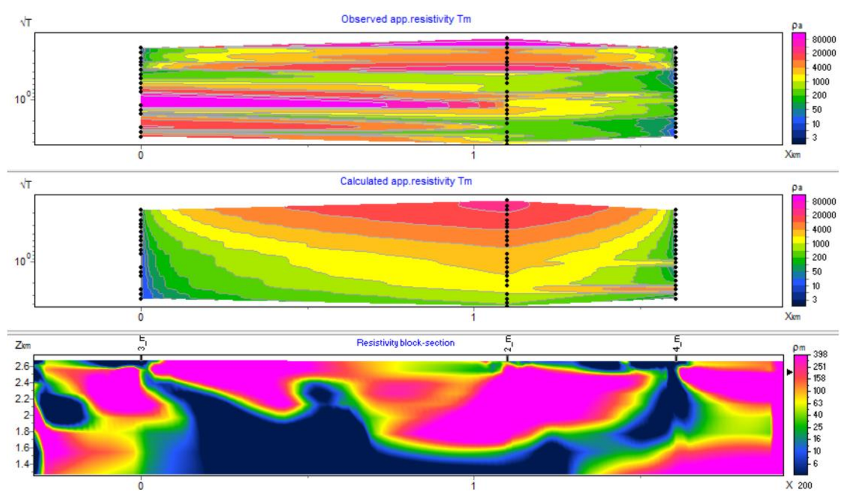

Figure A3 Processed data with no dome feature added, inverted with Occam method

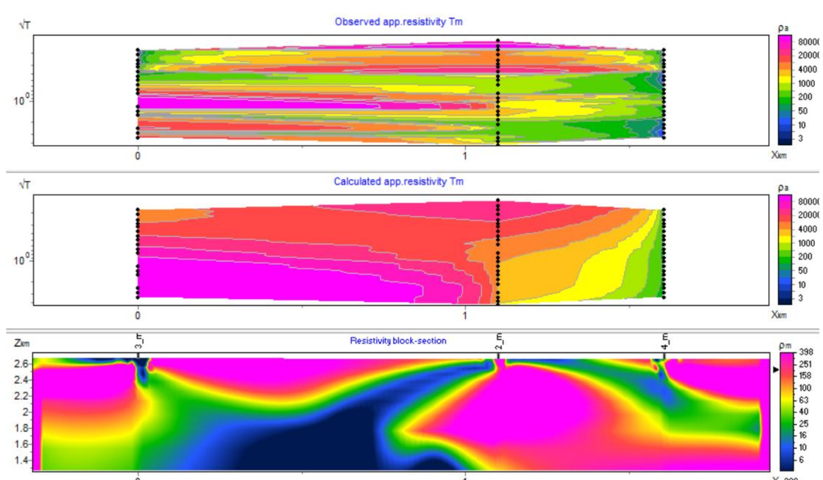

Figure A4 Semiprocessed data without Rico dome feature added, and Marquardt method used

A.2 Description of inversion methods

Occam Method

The Occam inversion method produces smooth models that fit the data of electromagnetic surveys. The smoothness depends of the number of rectangular elements manually added to the model mesh. Because smooth models are not always descriptive of the actual system, the Zond MT framework allows the user to add known sharp features. For more information on equations and methods, consult deGroot-Hedlin & Constable, 1990 (Occam's inversion to generate smooth, two-dimensional models from magnetotelluric data, http://marineemlab.ucsd.edu/resources/Pubs/OCCAM2D.pdf).

Marquardt Method

Algorithm that finds the least square fit for nonlinear solutions of data fitting for the model. Whereas Occam employs a smoothing constraint, the Marquardt uses a dampening factor to solve the non-unique data matrices. For more information, consult Widodo & Saputera, 2016 (Improving Levenberg-Marquardt Algorithm Inversion Result Using Singualr Value Decomposition, https://www.researchgate.net/publication/305800878_Improving_Levenberg-Marquardt_Algorithm_Inversion_Result_Using_Singular_Value_Decomposition).

A.3 ALS Radium test results

ALS -- Fort Collins **SAMPLE SUMMARY REPORT**

Client: Colorado School of Mines **Date:** *16-Aug-16*
Project: 1 Rico Geothermal **Work Order:** 1607368
Sample ID: Rico HS 1W **Lab ID:** 1607368-1
Legal Location: **Matrix:** WATER
Collection Date: 7/15/2016 14:00 **Percent Moisture:**

Analyses	Result	Qual	Report Limit	Units	Dilution Factor	Date Analyzed
Radium-226 by Radon Emanation - Method 903.1		**PAI 783**		Prep Date: **8/9/2016**		PrepBy: **CDJ**
Ra-226	**11 (+/- 2.8)**		**0.2**	**pCi/l**	NA	8/16/2016 12:30
Carr: BARIUM	*95.5*		*40-110*	*%REC*	DL = NA	8/16/2016 12:30

A.4 Resistivity results from 2016

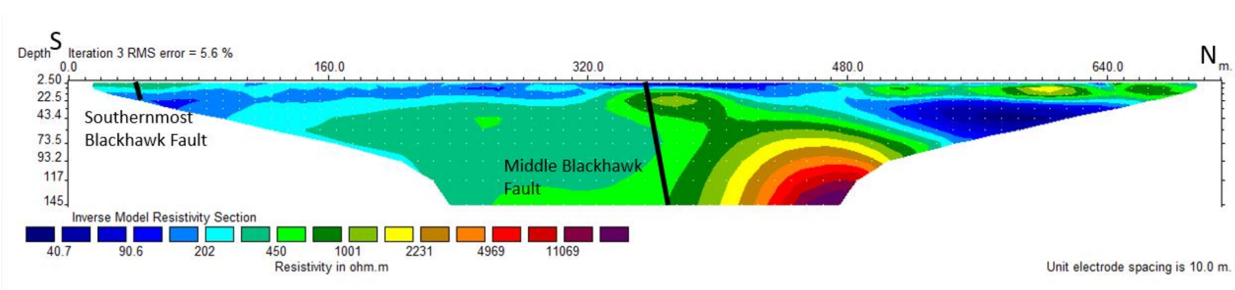

Figure A5 Resistivity results from Blackhawk Fault north of Rico along I-145

The suggested fault projections are presented as a result of in-field geologic observations as well as historic mapping in the region. To the north of the Middle Blackhawk Fault, the resistivity survey shows a highly resistive formation from about 43.3 m to the bottom of the survey's depth, represented by warmer colors on Figure A5. Between the two faults is large low resistivity region, represented by cool colors, which extends to the bottom of the survey.

Nontechnical Report Rico 2018

Prepared by Lucila Dunnington

In cooperation with Masami Nakagawa & Meghan Helper

June 26, 2018

Introduction

Rico has been identified by the Colorado Geological Survey for having a particularly promising geothermal resource, one of the few in Colorado. With the second highest heat flow in the state, and ample river resources feeding the reservoir, Rico is uniquely positioned to execute a successful geothermal project. Previous exploration trips have identified significant geologic faults in the region that potentially bound or feed the geothermal system below Rico: the Last Chance Fault just north of town diverts water down to the subsurface, and the Blackhawk fault near the National Forest information station provides a resistive boundary to the north.

A few crucial questions remained unanswered as of 2017; namely what is the depth of the reservoir, how much water does it contain, and what might the reservoir temperature be? These questions will never be fully known without a drilling program, but deep geophysical exploration can begin to answer these questions and better aim the exploration drill holes. Geophysics has been shown to improve the success rate of drilling by 30-40%. Since drilling can account for 30-60% of the entire cost of a geothermal project (about $150 per foot drilled, and increasing with depth), proper planning is critical.

Seismic and magnetotellurics (MT) are the two main deep geophysical methods used. MT has become dominant in the field of geothermal because it is inexpensive, portable in remote or rough terrain, and can distinguish well between water bearing rock and crystalline rock- which often serves as the heat source and cap rock in geothermal systems. MT operates by detecting natural electromagnetic signals of the Earth, making it a passive and very safe geophysical survey. However, because it relies on natural background signals, the survey is sensitive, and subject to common noise sources like traffic, powerlines, and even coiled metal wiring. It also requires a 100 m by 100 m flat expanse for setting out the cables, which is challenging in mountainous regions. Nevertheless, MT was selected as the deep geophysical exploration method for Rico.

Data Collection

The MT set-up centers on a recording system box at the survey site. At Rico, the recording system was connected to 4 electrode cables that extend in the north, south, east and west directions, and 2 magnetometer cables oriented parallel to the north-south and east-west cables. The electrodes at the ends of the cables were placed in deep enough holes in the ground to ensure adequate contact with the ground. Magnetometers also were placed in trenches that prevented them from moving in the wind.

While eight sites were scouted for potential MT surveys, only three could collect reliable and reasonably noise-free data. The three successful sites were near the pavilion, the water tower, and the western hot spring (Figure 1). While only a 4-6 hour collection time is required to explore the target depths at Rico (500-1000m), the collections times at the three sites were 6hr at the pavilion, 8hr at the water tower, and 6hr at the hot spring to acquire adequate data.

A short preliminary survey was taken before the full survey to check the ground contact and connectivity of the wires. If the survey pre-test failed, the cables were adjusted and/or the electrodes were dug deeper and sometimes coated with a bentonite-water mixture. Once the survey was collecting correctly, it was left alone to run for its programmed time.

Figure 1 Pink squares mark MT survey sites for 2018 Rico exploration

Results and Significance

Once the data was collected, it was processed to remove noisy and erroneous signals, then inverted so that frequency data was translated to resistivity at depth- the resistivity indicates the water content and type of rock present at depth. The data inversion can vary by user since different smoothing and dampening parameters are chosen based on the perceived quality of the data and prior knowledge of the subsurface (for instance from geological surveys). The data collected from Rico was tested with various inversion methods, dampening parameters and smoothing factors to ensure the consistency of the results.

The result given in Figure 2 included the added known Rico Dome, and results similar between all inversion trials. The cool dark colors are less resistive, water bearing zones, and the warm light colors are more resistive, water devoid zones, interpreted as crystalline rocks.

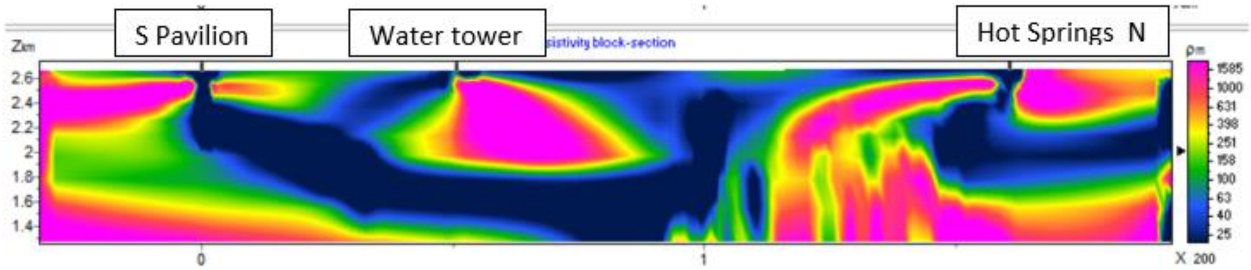

Figure 2 MT compilation and inversion of three survey sites, right is north, left is south, pink is high resistivity, blue is low resistivity, vertical axis is kilometers above sea level, horizontal axis is kilometers north of the pavilion

The result that persists through all trials of data inversion is the pond below the hot springs, from 500 to 1000m below the surface. This location is consistent with a permeable limestone layer known from the geologic record. If the Blackhawk and Last Chance faults are taken as the reservoir boundaries, and the water-bearing limestone layer is on average 30m thick, the geothermal reservoir is conservatively 75,000,000m^3. A 20% porosity limestone would yield 15,000,000m^3 of water. The lower part of the reservoir, 800- 1200 m deep, using the average geothermal gradient measured at the wells, should yield water of 81-121 degC, which agrees with reports from capped exploration wells of the area (Medlin, 1983).

Comparable systems in Colorado and World

While every geothermal system is hydrologically and geologically unique, as are the desires of the local people it might serve, established geothermal projects are presented in this section to illustrate the possibilities available from Rico's geothermal resource. With a million cubic meters of water, an observed artesian flowrate of 210 gallons per minute (gpm), and 100 degrees Celsius at less than a kilometer depth, Rico's resource is comparable to many in-use resources around the country and world.

Modoc County

In 2018, Modoc County became the sixth municipality in California to utilize geothermal energy for electricity production, and the first to use low temperature water. The breakthrough technology used, PwrCor™ is a modular scalable low-temperature power generator that can utilize water in the 80-100 degC range for energy production. It uses no fossil fuels or combustion, produces no emissions, and does not utilize flammable or harmful working fluids. Now in addition to having a rustic hot springs resort, it displays a new, sustainable way of producing electricity. Backed by a $2 million grant by the DOE, the plant's technology is "projected to produce 250 kW of electric power with 150 gallons per minute of water at 180 degrees F (82 degrees Celsius), enough power to service more than 150 homes" (Company release on Global Newswire). One module has a footprint of 5x10 feet according to a PwrCor spokesperson, and it utilizes a "closed loop" system, meaning the geothermal water is returned to the reservoir after heating the working fluid which transmits the heat energy to mechanical energy for electricity generation. The closed loop system does not deplete water in the reservoir, which is essential for water scarce regions. The community of Modoc County hopes to couple the electricity generation with cascading temperature usage schemes like a greenhouse or aquaculture to increase the value of their resource (Merrick, 2013).

Modoc County previously approved the use of 37 gpm well water at 87 degC to connect 34 buildings to a district heating project as well (MHA Environmental Consulting, Inc., 2003). The total project cost, which included retrofitting their old heating system, and constructing a laundry and food storage center, was $651,634. The school system that is connected to a geothermal district heating system is expected to save 70% on their annual $100,000 heating bill. The payback period for the project is an anticipated 7.5 years- high density towns, like Rico, can reduce the payback period for district heating to 4 years (EUDP, 2014).

Chena Hot Springs

The lowest temperature used for power generation from the Organic Rankine cycle to date is 73 degC in the Chena Hot Springs area in Alaska, which produces 400kW from two units (seen in Figure 3). Drawing 530 gallons per minute from their coastal reservoir, the technology called PureCycle-200 was designed with the aim to keep installation costs under $1300 per kW. The price of electricity generation per kilowatt-hour decreased from 30 cents to 5 cents for the rural Alaskan town (Chena Power, LLC.). The project cost a total of $2,007,770, funded in part by the Alaska Energy Authority, the AIDEA Power Project Loan Fund, and cash in kind contributions. The Chena Hot Springs power generation system won a Green Power Leadership Award from the EPA and DOE.

Figure 3 Two 225kW ORC Units at Chena Hot Springs, AK; Electricity from 73 degC warm water (from Holdmann, 2006)

The hot springs themselves have been used recreationally since 1905 by the miners in the area. Located 30 miles from the nearest power grid, Chena faces many problems shared by remote postmining communities: arduous maintenance of power lines, sparse phone and internet reception, underdeveloped sewage treatment system, limited access to road maintenance equipment, and limited access to emergency services. The cost of these essential services is augmented by the town's relative inaccessibility, having only one paved road.

Even with these limitations Chena is thriving due to extensive and efficient usage of their geothermal resource. While their geothermal upflow zone is only 0.02mi^2 (compared to Rico's 0.5mi^2) in areal extent with a discharge temperature of only 74 degC, the town has managed to develop district heating of 44 buildings, two geothermal greenhouses (the only commercial scale, year-round greenhouse in northern Alaska), a hot springs resort, and they produce their own electricity (Erkan et al., 2007). The district heating alone saved the town $183,000 in one year, while the electricity generation is estimated to save them $550,000 annually (Chena Power Company, 2007).

Pagosa Springs

The Pagosa district heating system utilizes water at 63 degC with a capacity of 1000gpm, though in winter months the maximum flowrate is typically 450gpm. The town boasts their heating costs are 25% less than gas heating and 30% less than electrical heating (www.pagosasprings.co.gov). The heat is diverted for use in the local Riff Raff Brewery and Pagosa Bakery.

Figure 4 Education Geothermal Greenhouse at Pagosa Springs during balloon festival

Pagosa Springs has also successfully completed a geothermal greenhouse which has been used for adult learning workshops, hands-on elementary education, and producing flowers and produce for the community (Figure 4). The objective of the first dome is to educate the community on sustainable horticulture, and "local energy" (Peterson, 2017). The project has also helped revitalize a previously downtrodden area near Pagosa's downtown. The dome structure is 42 feet in diameter, with a pool for thermal storage, and solar powered fans (Geothermal Greenhouse Partnership, 2014). While the business model includes selling produce to local restaurants, the greenhouse project is intended to be a non-profit endeavor. Each dome, developed by Pagosa's Growing Spaces, costs about $100,000.

Olkaria, Kenya

Sitting atop another rift system, Kenya has thoroughly developed its geothermal resource in the last 15 years. Now with six operational geothermal power plants, the Olkaria geothermal field has the capacity to produce double the country's peak electricity demand. The benefits cited by supporters of geothermal energy usage in Kenya are its small footprint, stability in price and production, and its benefit to the local community as electricity, infrastructure, and job generation (Lagat, 2010).

An associated health spa and demonstration center have been developed to display and promote the potential of direct use (i.e. non-electricity generating) geothermal energy projects. The spa uses about 1,300 gpm diverted from the 30-35 degC water at the outlet of the geothermal power plant to supply three large recreational ponds (diameters of 30m, 40m, and 70m). The water is then supplied to a greenhouse for heating and cooling. Nutrients from the water, namely hydrogen sulfide and carbon dioxide, further enrich the soil to improve flower yield (Mangi, 2013).

Conclusion

Currently there are about 800 district heating systems, thousands of developed natural hot springs and 563 Organic Rankine Cycle power plants worldwide (orc-world-map.org). These can run on a variety of low temperature resources, utilizing water-conserving, closed loop systems. The USDOE and NREL have traditionally been available to partly finance the development of rural renewable projects, and as technology has become more tested and reliable, green investors have grown too. The cost and payback of a geothermal project depends on the desires of the community, and their interest in cascading usage. Many of the cascade projects in place began with a single direct use application such as a spa, then expanded to district heating, and then to electricity generation. Direct-use projects generally have minimal start-up time, quicker return on investment, and can employ conventional (or non-specialized) equipment (Boyd, 2009). The costs of drilling, excavation and construction are more quickly offset if the geothermal heat is optimally scavenged, by linking usages in series, as in a combined heat and power project. Geothermal projects generally require a proposal and business plan, an environmental assessment, a feasibility study, and the acquisition of land and water rights- the details of this process are outside the scope of this paper, and the requisites vary depending on the scale and type of project.

The potential of geothermal energy is largely untapped in the world. While applications like heating and electricity generation are established, other applications like desiccation, desalination, water treatment, and horticulture are still in the early stages of development, and still other usages are undiscovered. Energy sovereignty, a growing phenomenon at the local level, has been proven to revitalize the economies, tourism, and beauty of rural communities. Based on the geophysical surveys, accounts of well bores, and data from other geothermal projects, Rico has the capability to produce local energy with its geothermal resource.

Acknowledgements

This research is supported by Durfee Day and the Town of Rico through the Mining and Earth Systems Engineering Department at the Colorado School of Mines. Many members of the Rico community and Colorado School of Mines community have been instrumental in the execution and success of this research including Barbara Betts, Kari Distefano, Linda Yellowman, Matt Wisniewski, and Brian Passerella.

References

Boyd, Tonya. (2009) Development of Direct Use Geothermal Projects. Geo-Heat Center, Oregon institute of Technology.

Chena Power Company. (2007) 400kW Geothermal Power Plant at Chena Hot Springs, Alaska: Final Report Prepared for Alaska Energy Authority.

Erkan K, Holdmann G, Blackwell D, & Benoit W. Thermal Characteristics of the Chena Hot Springs Alaska Geothermal System. Proceedings 32nd Workshop pn Geothermal Reservoir engineering, Stanford University, Stanford, California, January 22-24, 2007.

EUDP. (2014) Guidelines for Low-Temperature District Heating. Danish Energy Agency, Energiteknologisk Udviklings- og Demonstrations Program, EUDP 2010-II project Journal No. 64010-0479.

Geothermal Greenhouse Parnership. (2014) Business plan-September. Available at: Pagosagreen.org

Global Newswire. (January 9, 2018) PwrCor to Deliver its First Geothermal Powered Engine. https://globenewswire.com/news-release/2018/01/09/1285937/0/en/PwrCor-to-Deliver-its-First-Geothermal-Powered-Engine.html

Holdmann, Gwen. (2007) The Chena Hot Springs 400kW Geothermal Power plant: Experience Gained during the First Year of Operation. Chena Power, Fairbanks, AK. http://citeseerx.ist.psu.edu/viewdoc/download?doi=10.1.1.532.6994&rep=rep1&type=pdf

Lagat, John. (2010) Direct utilization of geothermal resources in Kenya. Proceedings World Geothermal Congress, Bali, Indonesia, 25-29 April 2010.

Mangi, Peketsa. (2013) Direct utilisation in Kenya: a case of a geothermal spa and demonstration centre at Olkaria. Olkaria Geothermal Project. Short Course VIII for Geothermal Resources, Lake Bogoria and Lake Naivasha, Kenya, Oct. 31-Nov. 22, 2013.

Medlin, Eric. (1983) Modeling local thermal anomalies: constraints from conductivity, gravity and heat flow. Master of Science Thesis, University of Wyoming.

Merrick, Dale. (2013) Canby Cascaded Geothermal Development Project: Phase 1 Feasibility Study. Geothermal Technologies Program- Low-Temperature Resources DE-EE0004431.

MHA Environmental Consulting, Inc. (2003) I'SOT Cnaby District Heating Project Modoc County, California, Final Environmental Assessment. DOE/EA 1460.

Peterson, Eric. (2017) Agriculture goes geothermal in Pagosa Springs. Coloradobiz, 2017.07.24.